

## Single Crystal $^{133}\text{Cs}$ NMR Study of $\text{Cs}^+(\text{15-Crown-5})_2\text{I}^-$

Kang Yeol Lee, Tae Ho Kim, Yong Woon Shin, and Jineun Kim\*

Department of Chemistry and Research Institute of Natural Sciences, Gyeongsang National University, Chinju 660-701, Korea

Received October 9, 2003

Cesium-133 NMR spectra of a single crystal of tetragonal  $\text{Cs}^+(\text{15-crown-5})_2\text{I}^-$  were obtained as a function of crystal orientation in an applied magnetic field of 9.40T and analyzed to provide the magnitudes and orientations of the  $^{133}\text{Cs}$  chemical shift and quadrupolar tensors for two magnetically nonequivalent and symmetry related sites. Chemical shift tensor components and parameters of quadrupolar interactions are obtained as  $\delta_{11} = 46$  (1),  $\delta_{22} = 60$  (1),  $\delta_{33} = -30$  (1) ppm, quadrupole coupling constant  $\text{QCC} = 581$  (1) kHz, and asymmetry parameter  $\eta = 0.481$  (1), respectively. The nonaxially symmetric NMR parameters imply that the local environment of the cesium nuclei is nonaxially symmetric. The DANTE experiment burned holes in the  $^{133}\text{Cs}$  NMR line of the title compound. The hole burning of the single crystal and powder  $^{133}\text{Cs}$  NMR lines showed that the NMR lines are not homogeneously broadened.

**Key Words** : Crown ether, Cesium, NMR, DANTE, Hole burning

### Introduction

The study of quadrupolar nuclei by NMR spectroscopy has been used to provide information on the electronic and structural properties of solids. The 100 % naturally abundant  $^{133}\text{Cs}$  nucleus with a nuclear spin of 7/2 is an attractive one for study as it has a relatively small quadrupole moment and a moderate chemical shift range sensitive to its environments. The complexation of the cesium cation by crown ethers or cryptands in aqueous and nonaqueous solvents have been studied by  $^{133}\text{Cs}$  NMR to understand the factors that control the thermodynamic and kinetic stability and selectivity of the resulting complexes.<sup>1-4</sup> There have been numerous applications of solid state  $^{133}\text{Cs}$  NMR to wide variety of chemical systems, such as inorganic salts,<sup>5-7</sup> clay minerals and glasses,<sup>8-10</sup> polymers,<sup>11</sup> and alkalides and electrides.<sup>12-15</sup>

The NMR peak in polycrystalline solids is remarkably broader than narrower lines in solution. This line broadening is primarily due to an orientation dependence of the magnetic field at the nucleus generated by anisotropic interactions. In order to obtain these anisotropic parameters, the lineshape analysis of static, MAS or variable angle spinning (VAS) NMR spectra at different magnetic fields are required. Analysis of NMR powder patterns arising from quadrupolar nuclei by spectral simulation is complicated because, in general, the lineshape will depend on both the magnitude and orientation of the nuclear quadrupolar (Q) and chemical shift (CS) interactions. In addition, other nuclei such as protons generate dipolar field at the  $^{133}\text{Cs}$  nucleus. Recent powder and single crystal  $^{133}\text{Cs}$  NMR study provided clear information on the magnitude and orientation of these interactions in  $\text{Cs}_2\text{CrO}_4$ .<sup>16,17</sup> Although a number of  $^{133}\text{Cs}$  NMR study of cesium complexes such as alkalides and

electrides have been made, the studies were limited on the magic angle spinning (MAS) NMR for identification of  $\text{Cs}^+$  and  $\text{Cs}^-$ .<sup>12-15</sup>

Maricq *et al.* have pointed that "when two or more interactions (chemical shift and dipolar) are present simultaneously, the result is inhomogeneous if any of the interactions is homogeneous".<sup>18</sup> In other words, if abundant spins (H) around the nuclei (Cs) to be studied are strongly coupled to each other, then the spin system being studied becomes homogeneous. The title compound could be a good example because there are a number of protons around cesium nuclei to be studied. The protons become homogeneous since they rapidly communicate each other owing to exchange their spins. The cesium nuclei become homogeneous via proton dipolar interaction. Then, the cesium-133 NMR line will be collapsed by the hole burning experiment, otherwise holes can be burn.<sup>19</sup>

Herein, we report static, MAS, and single crystal  $^{133}\text{Cs}$  NMR study of  $\text{Cs}^+(\text{15-crown-5})_2\text{I}^-$  and the result of the hole burning experiment.

### Experimental Section

The 15-crown-5 and cesium iodide were purchased from Aldrich and used as received. A polycrystalline sample of  $\text{Cs}^+(\text{15-crown-5})_2\text{I}^-$  was obtained by evaporation of methanol solution containing the stoichiometric amount of cesium iodide and 15-crown-5. The polycrystalline sample was dissolved in acetone and slow evaporation of the resulting solution gave single crystals of  $\text{Cs}^+(\text{15-crown-5})_2\text{I}^-$  suitable for single crystal NMR.

The powder and MAS NMR studies were carried out on a Bruker 400AM spectrometer equipped with a Bruker MAS probe. Hole burning and single crystal experiments were performed on a Varian VXR 400S spectrometer equipped with a Varian 5 mm wideline probe and a home-built single crystal probe the Max T. Rogers NMR facility at Michigan

\*Corresponding Author. Tel: +82-55-751-6024; Fax: +82-55-761-0244; e-mail: jekim@gsnu.ac.kr

State University. 10-20 repetition pulses with 0.8-1.2  $\mu\text{s}$  pulse length and 40-150  $\mu\text{s}$  delay times between the pulses were used for the DANTE experiment and the transmitter offset was centered on the central transition. All chemical shifts were measured respect to a value of 0 ppm for  $\text{Cs}^+(\text{aq})$  extrapolated to infinite dilution. A single crystal was mounted such that the crystal axes  $a$ ,  $b$ , and  $c$  coincide with the cube axes  $X$ ,  $Y$ , and  $Z$ , respectively.

Single crystal data were analyzed by using KINFIT<sup>20</sup> with Xtalnmr,<sup>21</sup> which is a Fortran program for calculating single crystal NMR transition frequencies. Powder pattern was calculated with the program VMAS.<sup>22</sup>

### Results and Discussion

A typical  $^{133}\text{Cs}$  NMR spectrum of the  $\text{Cs}^+(\text{15-crown-5})_2\Gamma^-$  single crystal is shown Figure 1(a). The spectrum consists of 14 resolved peaks. So far, we have not succeeded in solving the structure of this compound. However, its space group must be  $I4$  with the unit cell dimensions  $a = b = 13.173 \text{ \AA}$ ,  $c = 16.645 \text{ \AA}$  and  $Z = 4$ . The crown ether sandwich unit lies on a screw axis which requires successive complexed cations along the  $c$ -direction in the crystal to be rotated by  $90^\circ$  about the  $c$ -axis. Thus, two orientations of the sandwich units exist, which are equivalent crystallographically, but different magnetically. Two sets of 7 peaks are consistent with this. The crystallographically equivalent ions have identical chemical shift and quadrupole coupling tensors, hence only

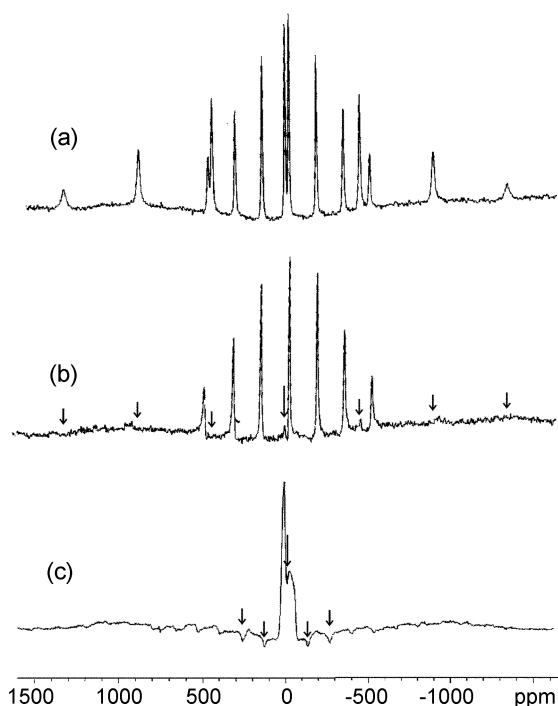


**Figure 1.**  $^{133}\text{Cs}$  NMR spectra of  $\text{Cs}^+(\text{15-crown-5})_2\Gamma^-$  (a) non-selective irradiation with a single crystal (b) selective saturation with the single crystal (delay time of 42.4  $\mu\text{s}$ ) and (c) selective saturation with a powder sample (delay time of 146  $\mu\text{s}$ ). Irradiated peaks were indicated by arrows. The transmitter offset was indicated by longer arrows.

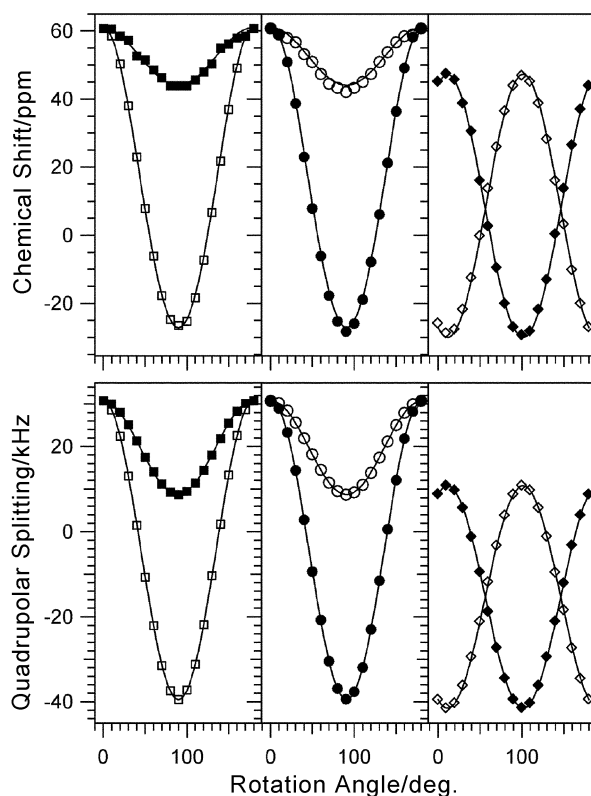


**Figure 2.** Single crystal  $^{133}\text{Cs}$  NMR data of  $\text{Cs}^+(\text{15-crown-5})_2\Gamma^-$  and least-squares curves for the central transitions (upper) and quadrupolar splittings  $\nu_Q$  (lower) ( $a$  axis;  $\square$ ,  $\blacksquare$ ,  $b$  axis;  $\circ$ ,  $\bullet$ ,  $c$  axis;  $\diamond$ ,  $\blacklozenge$ , site1; solid symbol, site2; open symbol).

one peak is observed in the MAS NMR (Fig. 3(a)).

Single crystal cesium-133 NMR spectra of  $\text{Cs}^+(\text{15-crown-5})_2\Gamma^-$  were obtained for rotations about the three orthogonal axes of the Kel-F cube mount. Rotations were performed about an axis perpendicular to the magnetic field. The relative positions of the central transitions and the first order splittings as a function of rotation angle are shown in Figure 2. The spaces between peaks with negligible second order shifts are nearly the same. Rotation plots indicate that the direction of the principal values of both the chemical shift tensor and the quadrupole coupling tensor are coincident. The central transition only depends on the chemical shift interaction, while the first order splitting depends on the quadrupolar interaction. In this paper, the first order splitting,  $\nu_Q = \nu_{m \rightarrow m-1} - \nu_{m-1 \rightarrow m-2}$  is the difference between resonance lines. The  $\nu_Q$  up to first order has only one value owing to negligible second order shift. The central transitions and the first order splittings were fit to the function,

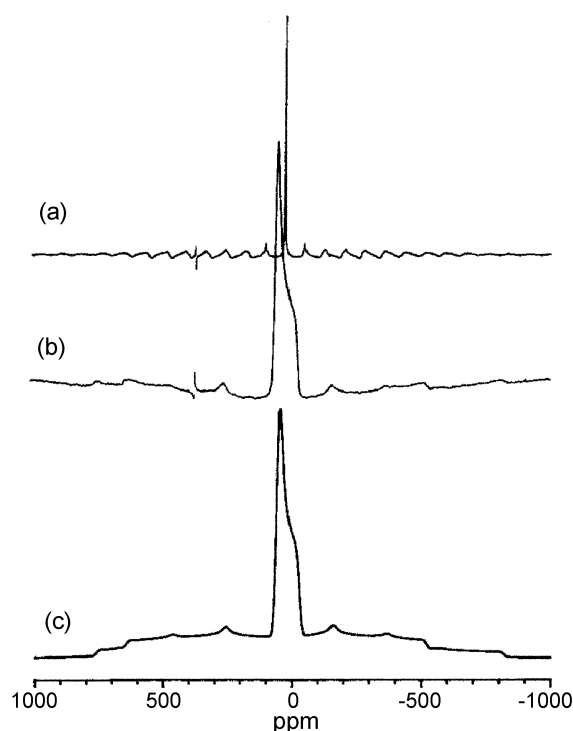
$$\nu(\nu)_i = A_i + B_i \cos 2\varphi + C_i \sin 2\varphi \quad (1)$$

where  $\varphi$  is the rotation angle,  $i = X, Y, Z$ , is the cube axis about which the rotation occurs. Diagonalization of these tensors yields the magnitudes of the interactions in their respective principal axis system (1, 2, 3), and more importantly, provides the direction cosines that describe the orientation of the principal axis system with respect to the cube frame. From the direction cosines, one can calculate

**Table 1.** Principal values of cesium-133 chemical shift (ppm) and electric field gradient ( $10^{21}$  V/m $^2$ ) tensors, and direction cosines and Euler angles ( $^\circ$ ) with respect to the cube frame

$\delta_{11} = 46$ $ V_{11}  = 2.08$	$\delta_{22} = 60$ $ V_{22}  = 5.93$	$\delta_{33} = -30$ $ V_{33}  = 8.01$
site 1		
0.017	-1.000	0.000
0.980	0.016	-0.197
0.197	0.003	0.980
$\alpha = 1.0$	$\beta = 11.4$	$\gamma = 270.0$
site 2		
-0.017	1.000	0.000
-0.197	-0.003	0.980
0.980	0.016	0.197
$\alpha = 1.0$	$\beta = 78.6$	$\gamma = 90.0$

the Euler angles ( $\alpha$ ,  $\beta$ ,  $\gamma$ ). Then,  $\nu(\varphi)_i$  for all transitions can be calculated to the equations in the literature<sup>22</sup> with the Euler angles and the principal values of both tensors. The second order shifts are included in the final calculation, which are less than 1 ppm. In this paper, total 30 multiple data set of 5 transitions ( $m = -5/2 \leftrightarrow 5/2$ ) were fit to the equations in the literature,<sup>22</sup> yielding principal values of both tensors and the Euler angles. Other two lines with the largest splitting are excluded in the fitting owing to the noise and broader linewidth. At this point, it was also useful to check the matching of the  $0^\circ$  and  $90^\circ$  values of the frequencies for the three sets of data and to use a small phase angle ( $\xi$ ) where slight differences in the frequencies. This angle indicates the error in attempting to align the single crystal in the cube frame. The phase angle for plots present here is  $\xi = 1.0(1)^\circ$ . This is a very small angle in comparison with those in the literature.<sup>17</sup> The values for the principal components of the chemical shift tensor are  $\delta_{11} = 46(1)$ ,  $\delta_{22} = 61(1)$ ,  $\delta_{33} = -30(1)$  ppm. The quadrupole coupling constant and the asymmetry parameter are  $\text{QCC} = 581(1)$  kHz and  $\eta = 0.481(1)$ , respectively. The principal components of electric field gradient tensor,  $V_{11}$ ,  $V_{22}$  and  $V_{33}$  can be calculated directly from  $\text{QCC} = e^2qQ/h = eQV_{33}/h$  and  $\eta = (V_{11} - V_{22})/V_{33}$  obtained with the experimental data. The resulting principal components of the chemical shift and electric field gradient tensors and direction cosines in the cube frame are given in Table 1. The principal components of chemical shift and electric field gradient tensor,  $\delta_{22}$  and  $V_{22}$ , respectively, lie along the crystallographic  $c$  axis. The other two components deviate  $11.4^\circ$  from the crystallographic  $a$  or  $b$  axes. Among these,  $\delta_{33}$  might direct close to a normal line to the crown ether ring plane, since  $\delta_{22}$  is parallel to the crown ether ring plane and the value of  $\delta_{22}$  is closer to that of  $\delta_{11}$  than that of  $\delta_{33}$ . The ring plane fits the crystallographic equation, in Ångstroms,  $-7.107x + 11.090y - 0.081z - 3.668 = 0$ , which is nearly parallel to the  $c$  axis.<sup>23</sup> In other words,  $\delta_{33}$  is located between  $a$  axis (or  $b$  axis) and the normal line to the crown ether ring plane. One might expect both the chemical shift and the quadrupole coupling tensors to be axially symmetric since the structure is tetragonal. However, the tensors with  $\eta$

**Figure 3.** Powder  $^{133}\text{Cs}$  NMR spectra of  $\text{Cs}^+(15\text{-crown-5})_2\Gamma^-$  (a) MAS (b) static (c) simulated spectrum with the single crystal data.

$= 0.481$  are nonaxially symmetric. This may result from the asymmetric local structure of the sandwich complexed cesium cation. Figure 3(b) show a static cesium-133 NMR spectrum of the powdered  $\text{Cs}^+(15\text{-crown-5})_2\Gamma^-$ , which agrees well with the simulated powder pattern (Fig. 3(c)) with the parameters obtained from the single crystal NMR data.

The single crystal  $^{133}\text{Cs}$  NMR lines have linewidth of 700-1000 Hz and proton decoupling removed most linebroadening. The lines are mainly broadened by dipolar interaction with protons and the residual linewidth with decoupling is about 100 Hz. Although the dipolar interaction is not strong, this can not be ignored. The selectively saturated cesium-133 NMR spectra by the DANTE pulse sequence are shown in Figure 1(b) and (c). The widths of selectively saturated lines become 400-2500 Hz, depending on the experimental conditions. Irradiated peaks are indicated by arrows. One of the two sets of single crystal cesium-133 NMR spectrum is clearly disappeared (Fig. 1(b)), which was selectively irradiated by the DANTE pulse. The other with smaller quadrupolar splitting remains unchanged. This implies that there is no energy transfer between two sites. If the powder line is homogeneously broadened, the intensity of the whole line will be decreased. However, a series of holes with even space are present in the powder pattern (Fig. 1(c)) in comparison with a normal powder line (Fig. 3(b)). The central line is characterized by CS interaction and a hole was burn as indicated by a longer arrow in Figure 1(c). The broad line outside of the central line is broadened by the quadrupolar interaction and has a series of holes. Some of the holes are indicated by arrows. This indicates that the energy, which was absorbed by one spin system, was not

transferred to another via protons. The cesium-133 NMR spectra of  $\text{Cs}^+(15\text{-crown-5})_2\Gamma^-$  are not homogeneously broadened. Therefore, the dipolar interaction is not strong enough to make both Cs sites homogeneous and the Maricq's usage cannot be applied to the spin system of the title compound.

### Conclusion

This study has shown that the cesium-133 NMR is a powerful technique to study chemical shift and quadrupolar interactions in  $\text{Cs}^+(15\text{-crown-5})_2\Gamma^-$ . The nonaxially symmetric NMR parameters show that the local environment of the cesium nuclei is more important rather than crystal symmetry.

**Acknowledgment.** The support of the Korea Research Foundation (2002-015-D00006) is gratefully acknowledged. We thank Professor J. L. Dye and Mr. J. Kermit at the Michigan State University for their assistance in obtaining the NMR spectra.

### References

1. Popov, A. I.; Lehn, J. M. In *Coordination Chemistry of Macrocyclic Compounds*; Melson, G. A., Ed.; Plenum: New York, 1979; p 537.
2. Izatt, R. M.; Pawlak, K.; Brashaw, S. J.; Bruening, R. L. *Chem. Rev.* **1991**, *91*, 1721.
3. Kim, J.; Shamsipur, M.; Huang, S. Z.; Huang, R. H.; Dye, J. L. *J. Phys. Chem. A* **1999**, *103*, 5615.
4. Meier, U. C.; Detellier, C. J. *Phys. Chem. A* **1999**, *103*, 3825.
5. Lim, A. R.; Han, O. H.; Jeong, S.-Y. *J. Phys. Chem. Solid* **2003**, *64*, 933.
6. Furukawa, Y. *J. Mol. Struct.* **1995**, *345*, 119.
7. Ikeda, R.; Ishimura, S.; Tanabe, T.; Nakamura, D. *J. Mol. Struct.* **1995**, *345*, 151.
8. Hunger, M.; Schenk, U.; Buchholz, A. *J. Phys. Chem. B* **2000**, *104*, 12230.
9. Luca, V.; Hanna, J. V.; Smith, M. E.; James, M.; Mitchell, D. R. G.; Bartlett, J. R. *Micropor. Mesopor. Mater.* **2002**, *55*, 1.
10. Click, C. A.; Brow, R. K.; Alam, T. M. *J. Non-Cryst. Solids* **2002**, *311*, 294.
11. Desolle, V.; Bayle, J. P.; Courtieu, J.; Rault, J.; Judeinstein, P. *J. Phys. Chem. B* **1999**, *103*, 2653.
12. Ellaboudy, A.; Dye, J. L.; Smith, P. B. *J. Am. Chem. Soc.* **1983**, *105*, 6490.
13. Dawes, S. B.; Ellaboudy, A.; Dye, J. L. *J. Am. Chem. Soc.* **1987**, *109*, 3508.
14. Dawes, S. B.; Eglin, J. L.; Moeggenborg, K. J.; Kim, J.; Dye, J. L. *J. Am. Chem. Soc.* **1991**, *113*, 1605.
15. Wagner, M. J.; Dye, J. L. *J. Solid State Chem.* **1995**, *117*, 309.
16. Power, W. P.; Wasylshen, R. E.; Mooibroek, S.; Pettitt, B. A.; Danchura, W. *J. Phys. Chem.* **1990**, *94*, 591.
17. Power, W. P.; Mooibroek, S.; Wasylshen, R. E.; Cameron, T. S. *J. Phys. Chem.* **1994**, *98*, 1552.
18. Maricq, M. M.; Waugh, J. S. *J. Chem. Phys.* **1979**, *70*, 3300.
19. Morris, G. A.; Freeman, R. *J. Magn. Reson.* **1978**, *29*, 433.
20. Dye, J. L.; Nicely, V. A. *J. Chem. Educ.* **1971**, *48*, 443.
21. Kim, J. Program Xtalnmr is available on E-mail request.
22. Kim, J.; Eglin, J. L.; Ellaboudy, A. S.; McMills, L. E. H.; Huang, S.; Dye, J. L. *J. Phys. Chem.* **1996**, *100*, 2885.
23. Dawes, S. B. *Ph. D. Dissertation*; Michigan State University: East Lansing, MI, 1986.